Preparation of C_2 Symmetric Transition Metal Complexes as Potential Chiral Catalysts

By

Lauren Jean Carlson

****

Submitted in partial fulfillment
of the requirements for
Honors in the Department of Chemistry

Union College

June, 2007

TABLE OF CONTENTS

ABSTRACT

CARLSON, LAUREN Preparation of C_2 Symmetric Transition Metal Complexes as Potential Chiral Catalysts. Department of Chemistry, June 2007.

Catalytic asymmetric synthesis is of great importance to the industrial production of biologically active substances such as pharmaceuticals, flavoring and sweetening agents, and insecticides. A special class of C_2 symmetric transition chiral metal complexes has proven very useful in catalytic asymmetric synthesis. Jacobsen's catalyst is a well-known C_2 symmetric transition metal chiral catalyst; however, the essential features of this catalyst are not clearly understood. In an attempt to determine more precisely the mechanism of catalysis, we have been synthesizing transition metal complexes with a chiral ligand of our own design. This ligand design employs a "bulky" spiro-backbone, a six-membered ring between the chelating nitrogens, and is expected to have an extreme tilt of the aromatic rings of the ligand. The first part of the synthesis is the preparation of the spiro[4,4]nonane-1,6-dione. A three-step synthesis has been used to prepare ~40 g of this intermediate in an overall 48% yield. The spirodiketone has been converted to (1S,5R,6S)-spiro[4.4]nonane-1,6-diol in 31% yield, and this diol was converted to the diazide via the corresponding dimesylate. Hydrogenation of the diazide has provided the desired (1R,5R,6R)-spiro[4.4]nonane-1,6-diamine which was reacted with 2-hydroxybenzaldehyde in a condensation reaction to form the tetradentate ligand. Future plans include chelation of the ligand to manganese (III), cobalt (II), and chromium (III). These corresponding complexes will be fully characterized and studied for catalytic reactivity in the asymmetric synthesis of substrates similar to that of Jacobsen's catalyst.

INTRODUCTION

The ability to synthesize chiral molecules from non-chiral substrates is of great importance to synthetic organic chemistry. Catalytic asymmetric synthesis is a method that has recently experienced great success in synthesizing large enantiomeric excesses of chiral molecules. C_2 symmetric transition metal complexes have proven to be unusually good catalysts for this. Despite the success of the current catalysts in this class, there is a desire to synthesize new catalysts with higher selectivities and that will work on a wider range of substrates. The principles behind chirality, in addition to studies carried out on previous chiral catalysts, offer insight into the requirements for a catalyst to be successful.

Chirality and Chiral Molecules

Chirality is a stereochemical property in which an object, such as a molecule, is non-superimposable on its mirror image. The term chiral comes from the greek word "cheir" meaning hand. Like right and left hands, chiral molecules come in mirror image pairs. These pairs are known as enantiomers. One distinct property of each enantiomer is its ability to rotate plane polarized light. The different enantiomers of the same molecule rotate light in opposite directions, which gives rise to no net rotation if they are present in equimolar amounts. When both enantiomers are found in equimolar amounts, the mixture is referred to as racemic. A racemic mixture can have different physical properties from that of each individual enantiomer, such as melting point, while each enantiomer has equivalent chemical and physical properties when in *symmetric environments*.

Chirality is present throughout nature and can be seen in natural objects such as the human body, helical seashells, sugars, DNA, and amino acids. Many biological receptors are also chiral. When the enantiomers of a chiral molecule interact with a chiral receptor, the molecule can be thought of as a hand and the receptor as a glove. Each enantiomer represents a different hand, and only one hand fits in the glove. This sort of selective interaction between a particular enantiomer and a *chiral environment* results in the different chemical and physical properties between enantiomers. When the wrong enantiomer interacts with a chiral molecule receptor, the interaction can have any number of outcomes, some without incident and others with destructive results.

Limonene is an example of a chiral compound that interacts with chiral nasal receptors resulting in different responses. The (*S*)-limonene form gives rise to the scent of lemons while the (*R*)-limonene smells of oranges. As can be seen in Figure 1, these two compounds are mirror images of each other and are differentiated in naming by the (*R*)- and (*S*)- designation. The (*R*)- and (*S*)- designations are made based on assigning priority to substituents at the chiral center using Cahn Ingold Prelog priority rules. Enantiomers can also be distinguished by a (+)- and (-)- naming system. The (+)- and (-)- designations are made based on the direction in which the enantiomer rotates plane polarized light. These two naming systems are commonly used but there is no relation between the two systems. For example, a molecule that is given the (*S*)- designation could have either the (+)- or (-)- designation.

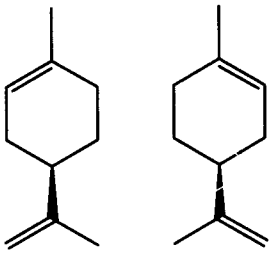

Figure 1. *Structures of each limonene enantiomer.*

While the differences between enantiomers of limonene are interesting, the differences between the enantiomers of thalidomide are dangerous. Thalidomide was a racemic drug that was sold in the 1950's and 1960's to combat morning sickness in pregnant women. However, many of the children of these pregnant women taking thalidomide were born with malformities. It was later discovered that (*S*)-thalidomide was responsible for alleviating morning sickness while (*R*)-thalidomide was causing the birth defects. A possible solution to this problem would be administering only one enantiomer; however, with thalidomide it has been discovered that the two enantiomers are intercoverted *in vivo*.

Because of problems due to differing enantiomer activity in racemic drugs, similar to those seen with thalidomide, it is generally desirable for drugs to be a single enantiomer. There are several ways that molecules can be synthesized to create this desired enantiomeric excess (ee). Enantiomeric excess is a percentage related to the percent excess of one enantiomer. For example, a sample with a 50% ee in S is 75% enantiomer S and 25% enantiomer R. In other words, 50% of the sample is racemic and 50% is of the excess pure enantiomer S. This value can be calculated either from the specific rotation of a sample or from when the moles of each enantiomer are known.

The first method for obtaining a high ee is to start from chiral starting material. From there, specific synthetic routes can be used that allow for the retention of chirality. When a product can be synthesized from a relatively common or inexpensive starting material such as sugars or amino acids this is a very attractive synthetic method. However, this method is often undesirable because appropriate chiral starting materials

are not always available and can be expensive. The limited choice of starting materials limits the reaction pathways as well.

A second option is selective separation. Here normal synthetic pathways are followed and the racemic product that results is separated into the corresponding enantiomers by using methods such as chromatography and recrystalization. These methods are often very difficult, but even when they are effective, at least half of the product is lost increasing the expense and creating large amounts of waste.

A final option is to use catalytic asymmetric synthesis. This method uses a chiral catalyst that leads to the preferential formation of one enantiomer.

Chiral Catalysts

The principle behind catalytic asymmetric synthesis is that a small amount of catalyst with enzyme-like selectivity can be used to generate a large amount of chiral product. In most catalysts, the metal center is responsible for transferring chirality to the desired molecule. For example, during chiral hydrogenation the H_2 and substrate bind to the metal center simultaneously. The reaction proceeds by H_2 addition to the double bond and then the chiral product is released from the catalyst so that another substrate can bind and react. It is during the hydrogenation step that it is possible for the H_2 to add in two different ways to form the different enantiomers. The reason that enantiomeric excess can be achieved with this method is based on the energy differences between the two different pathways. The transitions states for each of these pathways are not mirror images and therefore have different energies resulting in an excess of the product formed with the lower energy transition state.[1] Utilizing knowledge of this energy difference

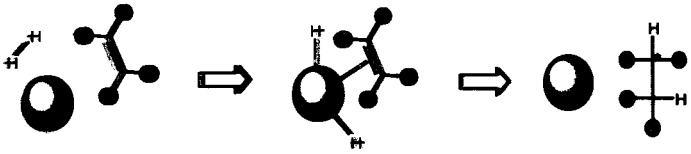

Figure 2. *Generic chiral hydrogenation scheme showing both the substrate and the hydrogen bound to the catalyst simultaneously, and then the release of the chiral product.*

makes it possible to increase the difference in energy between the transition states in order to obtain a larger excess of one enantiomer over the other.

C_2 Symmetric Transition Metal Complexes

In the area of catalytic asymmetric synthesis, C_2 symmetric transition metal complexes have proven to be quite successful catalysts. In fact, three scientists were awarded the 2001 Nobel Prize in Chemistry for their use of C_2 symmetric transition metal complexes in asymmetric syntheses. These scientists were William S. Knowles, Ryoji Noyori, and K. Barry Sharpless. Their work in asymmetric syntheses has proven very beneficial to both academic research and industrial synthesis.

DiPAMP

In 1968, William S. Knowles of the Monsanto Company in St. Louis, MO developed the first catalytic asymmetric hydrogenation. Knowles designed a catalyst based on two relatively recent discoveries at the time. The first was that of Osborn and Wilkinson who synthesized a soluble rhodium complex ligated to three triphenylphosphine molecules and one chloride ion. The solubility of this complex was key to its success catalyzing a hydrogenation in solution.[1] This complex however

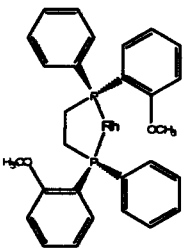

Figure 3. *Knowles' DiPAMP rhodium complex.*

was not chiral, so Knowles looked to the work of Horner and Mislow who had successfully synthesized chiral phosphines.[1] Knowles envisioned that perhaps by employing a chiral phosphine ligand bound to a transition metal such as rhodium, it may be possible to catalyze an asymmetric hydrogenation. The phosphine Knowles first tried was not enantiomerically pure but still showed catalytic ability in asymmetric hydrogenations.[1]

Knowles's goal was to develop an industrial synthesis of L-DOPA, an amino acid that had recently become known for its use in the treatment of Parkinson's disease. In the initial attempts at developing a good chiral catalyst, the Monsanto group synthesized a number of chiral phosphine ligands. Several of the ligands (such as CAMP (88% ee) and PAMP (58% ee)) showed enzyme like selectivity. The ultimate catalyst consisted of a chelating biphosphine ligand that contained two PAMP groups known as DiPAMP. With slightly higher ee (95%) and easier synthesis than CAMP, the Monsanto group chose to use the air stable crystalline DiPAMP solid for the industrial synthesis of L-DOPA.[2]

BINAP

Ryoji Noyori furthered the research of Knowles and others and developed better and more general catalysts for chiral hydrogenations. It was in 1980 that Noyori published the synthesis of both enantiomers of the diphosphine ligand BINAP. This particular ligand, when complexed with rhodium, could be used in the synthesis of certain amino acids with an ee close to 100%. Takasago International uses BINAP rhodium complex in the industrial synthesis of menthol, a chiral aroma substance. In the end, Noyori created a more general catalyst than that of Knowles. He did this by

substituting the rhodium (I) with ruthenium (II). This change resulted in the BINAP complex being able to hydrogenate functional groups other than alkenes such as ketones in high ee's. This ruthenium complex was used on an industrial scale for the synthesis of levofloxacin, an antibacterial.[3]

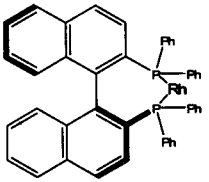

Figure 4. *Noyori's BINAP rhodium complex.*

BET

Barry Sharpless made further advances in the area of asymmetric synthesis by developing a catalytic method for the chiral synthesis of epoxides employing asymmetric oxidations of allylic alcohols. The catalyst he used forms in solution between titanium tetraisopropoxide and diethyl tartrate. The titanium simultaneously binds the hyperperoxide, chiral ligand, and substrate to form the catalyst and chiral epoxides. Chiral epoxides are very useful as intermediates in the syntheses of other chiral products such dialcohols, aminoalcohols, and ethers. Sharpless' chiral epoxidation is used to synthesize (*R*)-glycidol and is also used in the synthesis of beta-blockers by pharmaceutical companies.[4]

Jacobsen's Catalysts

Another well-known C_2 symmetric transition metal chiral catalyst is Jacobsen's catalyst. This catalyst uses Mn(III) complexes of chiral Schiff bases for enantioselective epoxidation of alkyl- and aryl-substituted olefins. Jacobsen's catalyst was originally synthesized in an attempt to make a more versatile catalyst by lifting restrictions on substrates to have specific functional groups (for example, allylic alcohols as required for

a Sharpless epoxidation) by having stereoselectivity rely solely on nonbonded interactions.[5] To some degree, Jacobsen's first catalyst was successful at achieving this by recording some of the highest selectivities on a variety of substrate substitution patterns.

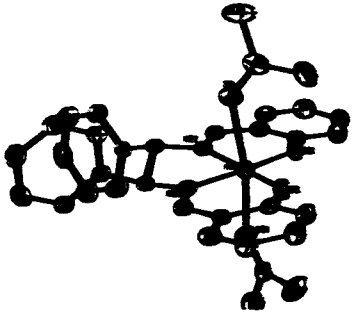

Figure 5. *X-ray crystal structure of an early form of Jacobsen's catalyst*

A later version of Jacobsen's catalyst was found to be even more selective than the first. The change in reactivity was a result of a) modifying the bridging diamine backbone and b) adding *t*-butyl groups to improve the solubility. Although the newer version of Jacobsen's catalyst worked well on *cis* olefins, its use on *trans* olefins yielded poor results.[6]

In order to design more selective asymmetric catalysts, it is necessary to increase the energy difference between the transition state complexes so that larger enantiomeric excesses can be achieved. In an attempt to uncover the reactive transition complexes and determine more precisely the mechanism of catalysts like Jacobsen's, Fristrup *et al.* recently studied the reactivity/selectivity of the Jacobsen-Katsuki epoxidation.[7] The results of their research suggest that there are competing pathways between two different approaches of the alkene to the catalyst and that the preference for one path over the other is affected by the inherent selectivity of each path.

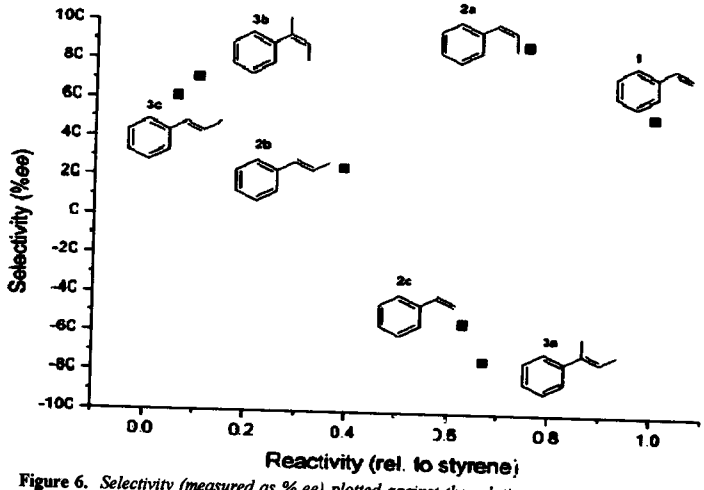

Figure 6. *Selectivity (measured as % ee) plotted against the relative reactivity (measured in competition with styrene). Positive ee values denote formation of the (R)-configuration at the benzylic position as the major product and negative ee values, the (S)-configuration.*

Current Research

Based on the knowledge of previous chiral catalysts and their selectivities, we have designed a chiral catalyst of our own. The catalyst consists of a tetradentate ligand with a spiro group backbone which contains two imine nitrogen donors and two phenolate oxygen atoms. Future work will include the synthesis of the corresponding Mn(III), Co(II), and Cr(III) complexes with this ligand. It is our expectation that these complexes will have reactivity similar to that of Jacobsen's catalyst. Simple energy minimization using Spartan suggests that the complexes will be similar to Jacobsen's but that the aromatic rings will be tilted at an even more extreme angle. This tilting is thought to be partly responsible for the chiral selectivity seen with Jacobsen's catalyst.[8]

In analogy with previously reported catalysts, we expect that these complexes should be capable of catalyzing the epoxidation of prochiral alkenes as well as some typical Lewis acid catalyzed reactions (for example, epoxide openings or Diels-Alder reactions). Once we have established that we have an active catalyst, we will compare our results with previous catalysts and then study the effect that changes to our catalyst have on its reactivity and chiral selectivity.

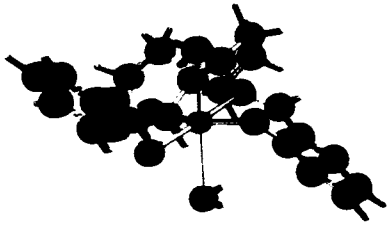

Figure 7. Proposed Co (II) complex with standard ligand framework

EXPERIMENTAL

Nuclear magnetic resonance (NMR) spectra were obtained on a Varian Gemini 200 NMR (^{1}H 200 MHz, ^{13}C 50.28 MHz) spectrometer. Sample spectra were taken in solvent denoted. Chemical shifts (ppm) are reported in reference to TMS (0.000 ppm) for ^{1}H NMR and respective internal references for ^{13}C NMR. Infrared (IR) spectra were obtained from a Thermoelectron Avatar 330 FT-IR spectrophotometer equipped with a Smart Orbit reflectance insert, diamond window. Mass spectra (MS) were recorded on a Hewlett Packard 5890A GC/MS. X-ray crystals structures were determined by Dr. Joseph M. Tanski of Vassar College on a Bruker APEX 2 CCD platform diffractometer (Mo Kα (λ = 0.71073 Å)) equipped with an Oxford liquid nitrogen cryostream. Crystals were mounted in a nylon loop with Paratone-N cryoprotectant oil. All reagents and

solvents were purchased from Sigma-Aldrich. Anhydrous solvents were obtained from Sigma-Aldrich.

Ethyl 1-(4-ethoxy-4-oxobutyl)-2-oxocyclopentanecarboxylate

A batch of 5.7 g 60% dispersion (143 mmol) sodium hydride was added to a dry, 3-neck, 250 mL round bottom flask. The flask was placed in an ice bath followed by the addition of 70 mL of anhydrous DMF. To the stirring mixture, 22.0 g (134 mmol) of ethyl 2-cyclopentanonecarboxylate were added dropwise. Following this addition, the mixture was left to stir for 5 min before adding 28.5 g (139 mmol) of ethyl 4-bromobutyrate dropwise. The round bottom flask was then removed from the ice bath and placed in a ~50° C water bath to stir for 2 h. The reaction was cooled to room temperature. Next, 300 mL of water and ~4 mL of acetic acid were added and the mixture was extracted with 150 mL of methyl *tert*-butyl ether (MTBE). The aqueous phase was extracted again with 100 mL of MTBE. The MTBE portions were combined and washed with 100 mL of brine. MTBE was removed via rotary evaporation, and the crude product was obtained in theoretical yield, but also contained excess ethyl 4-bromobutyrate and solvent. Yield 37.5 g (>100%). ^{1}H NMR ($CDCl_3$) 4.136 (m, 4H), 2.508 (m, 2H), 2.294 (m, 3H), 1.955 (m, 4H), 1.597 (m, 3H), 1.240 (t, 6H); IR 1725.21 cm^{-1}; Mass spectrum 270, 242, 224, 156.

4-(2-Oxocyclopentyl)butanoic Acid

A combination of 150 mL of concentrated hydrochloric acid and 150 mL of water were added to 40 g (134 mmol) of crude 4-(1-ethoxycarbonyl-2-

oxocyclopentyl)butanoate in a 500 mL round bottom flask equipped with a reflux condenser. The mixture was refluxed for 20 h, and then a Dean-Stark trap was added and ~50 mL of solvent were distilled off to remove the by-product ethanol. The mixture was then allowed to cool to room temperature, and 100 mL of brine were added. The mixture was then extracted with 100 mL of MTBE three times. The MTBE phases were combined and extracted with 150 mL of 1 M aqueous sodium hydroxide followed by a second extraction with 100 mL of 1 M sodium hydroxide. The two aqueous extracts were combined in a 1000 mL Erlenmeyer flask and cooled in an ice bath. Next, 100 mL of 3 M hydrochloric acid and 150 mL of MTBE were added to the flask. The cold solution was transferred to a separatory funnel and the aqueous phase was extracted two more times with 100 mL of MTBE. The MTBE phases were combined, and the solvent removed. Yield: 18.346 g (77 %). IR 1705.13 cm^{-1}; Mass spectrum 170, 152, 97, 84.

Spiro[4.4]-nonan-1,6-dione

To a 500 mL round bottom flask, 2.36 g (43 mmol) of crude 4-(2-oxocyclopentyl) butanoic acid and 300 mL of toluene were added. The volume was reduced until ~20 mL of solvent was removed. Then 4.11 g of para-toluenesulfonic acid monohydrate were added to the mixture. The round bottom was equipped with a Dean-Stark trap, and the mixture was refluxed for 24 h. The mixture was cooled to room temperature and solid sodium bicarbonate was added. After stirring for 10 min, 50 mL of saturated sodium bicarbonate and 50 mL of water were added. The phases were separated, and the aqueous phase extracted with 200 mL of MTBE. The combined organic phases were washed with brine, and the solvent was removed via rotary evaporation. The crude

mixture was then distilled using a short path distillation apparatus under vacuum to isolate the pure white solid (~1 mm Hg, b.p. 65-75 °C). Yield: 4.2 g (64 %). ^{1}H NMR ($CDCl_3$) 2.341 (m, 6H), 2.220 (m, 2H), 1.878 (m, 4H); ^{13}C NMR ($CDCl_3$) 216.824, 64.346, 38.428, 34.274, 19.831; IR 1712.61 cm^{-1}; Mass spectrum 152, 97.

***B*-n-butyl oxazaborolidine**

A 25 mL round bottom flask was charged with 0.500 g (1.97 mol) of (S)-(-)-α,α-diphenyl-2-pyrrolidinemethanol and 0.241 g (2.37 mol) of butylboronic acid. These reagents were dissolved in 15 mL of toluene and a Dean-Stark trap-like apparatus with refluxed condenser was attached. The trap of the apparatus was filled with ~12mL of toluene so the solvent level was near the joint. The mixture was refluxed for 8 h and then the solvent was removed *in vacuo*. Yield: 0.134 g (26 %). ^{1}H NMR ($CDCl_3$) 7.562 (m, 5H), 7.285 (m, 5H), 4.273 (t, 1H), 2.954 (q, 2H), 1.693 (m, 4H), 1.275 (m, 6H), 0.830 (m, 3H).

(1*S*,5*R*,6*S*)-Spiro[4.4]-nonane-1,6-diol

First, 1.92 g (6 mmol) of *B*-n-butyl oxazaborolidine were dissolved in 66.0 mL (66 mmol) of 1 M borane-THF complex in a 250 mL round bottom flask. The mixture was cooled to 0° C in an ice bath. Separately, 10.00 g (65.8 mmol) of spiro[4.4]-nonan-1,6-dione were dissolved in 40 mL of anhydrous THF. The spiro[4.4]-nonan-1,6-dione mixture was added to the *B*-n-butyl oxazaborolidine mixture over 15 min using an addition funnel. The resulting mixture was then stirred for 15 min, and then, very slowly, ~30 mL of anhydrous methanol were added to the mixture. The mixture was rotovapped

until ~30 mL of solvent had been removed. An additional 100 mL of anhydrous methanol were added followed by complete removal of the solvent, first with the rotovap and then *in vacuo*. Next, the product was dissolved in 100 mL of ethyl acetate, and 3 mL of 3 M hydrochloric acid were added to the solution. The flask was then placed in an ice bath for 15 min after which a white precipitate formed. The solid was filtered off and washed with cold ethyl acetate. The receiving flask was changed, and the crystals were washed with 15 mL of hexane. These crystals were the hydrochloride salt of (S)-(-)-α,α-diphenyl-2-pyrrolidinemethanol. They were saved, and can be used to regenerate the *B*-*n*-butyl oxazaborolidine. From the first receiving flask, the ethyl acetate mixture was washed with brine. The solvent was removed via rotary evaporation, and the resultant product was dissolved in 25 mL of methylene chloride and left in the refrigerator for 24 h. The white (1*S*,5*R*,6*S*)-spiro[4.4]-nonan-1,6-diol crystals that formed were filtered and dried. The solid was then recrystalized in methylene chloride. The ^{1}H NMR suggested the isolation of a single product. Yield: 3.18 g (31 %). ^{1}H NMR ($CDCl_3$) 3.812 (q, 2H), 2.026 (m, 2H), 1.621 (m, 12H); IR 3210.9 cm^{-1}; Mass spectrum 138, 120, 94.

(1*S*,5*R*,6*S*)-Spiro[4.4]-nonan-1,6-dimesylate

A 25 mL round bottom flask was charged with 1.05 g (6.73 mmol) of (1*S*,5*R*,6*S*)-spiro[4.4]-nonan-1,6-diol. The spirodiol was dissolved in 15 mL of anhydrous THF. The flask was then placed in a 0° C ice bath and purged with N_2 gas. Next, 3.75 mL (26.92 mmol) of triethylamine were added. After stirring for 5 min, 1.15 mL (14.81 mmol) of methanesulfonyl chloride were added *very* slowly over 20 min. The mixture was then left to stir air free in the ice bath. After 2 H, 50 mL of water were added to the mixture

and then it was extracted twice with 25 mL portions of MTBE. The organic phase was then washed with brine, and the solvent removed. Upon sitting a white solid formed, and the dimesylate was isolated in quantitative yield. ^{1}H NMR ($CDCl_3$) 4.776 (t, 2H), 3.059 (s, 6H), 1.743 (m, 12H).

(1*R*,5*R*,6*R*)-Spiro[4.4]-nonan-1,6-diazide

First, 0.399 g (1.28 mmol) of (1*S*,5*R*,6*S*)-spiro[4.4]-nonan-1,6-dimesylate were added to a 25 mL round bottom flask, and 5 mL of anhydrous DMSO were added to it. Then, 0.25 g (3.84 mmol) of sodium azide were added to the flask, and the mixture was left to stir in an ~80° C oil bath. After 24 h, the flask was removed from the oil bath and cooled to room temperature, and 35 mL of water were added to it. The mixture was then extracted twice with 15 mL portions of MTBE. The organic phase was then washed with brine, and the solvent removed. The product was then extracted into 7 mL of hexane, and concentrated on the rotovap again. The desired diazide was separated from a monoalkene/monoazide side product through column chromatography, eluting with hexane. The fractions containing the diazide were concentrated using the rotovap, and the remaining solvent was removed *in vacuo*. Yield: 0.075 g (29%). ^{1}H NMR ($CDCl_3$) 3.793 (s, 2H), 1.863 (m, 8H), 1.434 (m, 4H); ^{13}C NMR ($CDCl_3$) 70.325, 69.658, 32.904, 30.127, 20.901; Mass spectrum 206, 178, 122, 96, 67.

(1*R*,5*R*,6*R*)-Spiro[4.4]-nonan-1,6-diamine

A 10 mL round bottom flask was charged with 0.557 g (2.70 mmol) of (1*R*,5*R*,6*R*)-spiro[4.4]-nonan-1,6-diazide. The diazide was then dissolved in 8 mL of

methanol, and then two spatulas full of palladium, 5 wt. % (dry basis) on activated carbon, wet, Degussa type E101 was added to the flask. The flask was kept under hydrogen gas for 3 h. The palladium on carbon catalyst was filtered off, and the majority of the solvent was removed. Yield: 0.530 g (>100 %). ^{1}H NMR ($CDCl_3$) 3.550 (t, 2H), 1.801 (m, 8H), 1.440 (m, 4H); ^{13}C NMR ($CDCl_3$) 59.488, 50.967, 35.155, 34.775, 21.042; IR 2944.01 cm^{-1}, 2867.50 cm^{-1}, 1445.83 cm^{-1}; Mass spectrum [illegible]

2,2'-(1E,1'E)-(1S,5S,6S)-spiro[4.4]nonane-1,6-diylbis(azan-1-yl-1-ylidene)bis(methan-1-yl-1-ylidene)diphenol (SNIP)

First, 0.042 g (2.70 mmol) of (1*R*,5*R*,6*R*)-spiro[4.4]nonane-1,6-diamine were added to a 25 mL round bottom flask. The diamine was dissolved in 5 mL of anhydrous ethanol, and 0.890 mL (8.49 mmol) of salicylaldehyde were added to the solution. The yellow mixture was stirred for 45 min. The spindly yellow crystals that formed were filtered, and the remaining mother liquor was kept at 5°C overnight. The remaining solid that formed was filtered. Then the two batches of isolated crystals were combined and dried. Yield: 0.550 g (52 %). ^{1}H NMR ($CDCl_3$) 13.687 (s, 2H), 7.960 (s, 2H), 7.259 (m, 2H), 6.931 (d, 2H), 6.719 (m, 4H), 3.511 (d, 2H), 1.864 (m, 12H).

RESULTS AND DISCUSSION

Ethyl 1-(4-ethoxy-4-oxobutyl)-2-oxocyclopentanecarboxylate: Synthesis and Identification

The first molecule synthesized was ethyl 1-(4-ethoxy-4-oxobutyl)-2-oxocyclopentanecarboxylate. As seen in Reaction 1, this molecule was synthesized by

combining ethyl 2-cyclopentanonecarboxylate and ethyl 4-bromobutyrate in the presence of sodium hydride in DMF a procedure similar to that utilized by Nieman and Keay.[9]

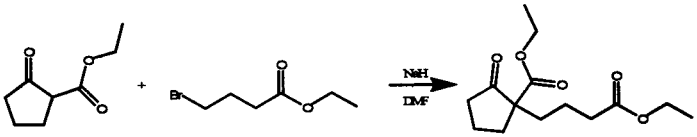

Reaction 1. *Synthesis of ethyl 1-(4-ethoxy-4-oxobutyl)-2-oxocyclopentanecarboxylate.*

Mechanistically, the first step of the reaction involves the base-catalyzed enolization of the ethyl 2-cyclopentanonecarboxylate. The enolate ion is in resonance with a carbon anion on either carbon adjacent to the ketone; however, in this case, the more substituted carbon stabilizes the charge through resonance with the ester group and is therefore more reactive. This nucleophilic carbon displaces the bromide of the ethyl 4-bromobutyrate forming the desired product.

For the synthesis of ethyl 1-(4-ethoxy-4-oxobutyl)-2-oxocyclopentanecarboxylate, it was important to use dry glassware and anhydrous solvents because sodium hydride can ignite when in contact with water. Upon the addition of ethyl 2-cyclopentanonecarboxylate to the sodium hydride slurry, it was important to vent the flask due to the production of hydrogen gas. Also, following the addition of ethyl 4-bromobutyrate, it was not uncommon for the mixture to become cloudy and viscous. Additional DMF could be added to regain th more homogenous and fluid light orange solution. The calculated yield was always greater than the theoretical yield for this reaction because excess ethyl 4-bromobutyrate remained even after the workup. Completion of the reaction could be followed by GC-MS through the disappearance of the ethyl 2-cyclopentanonecarboxylate and the appearance of the product.

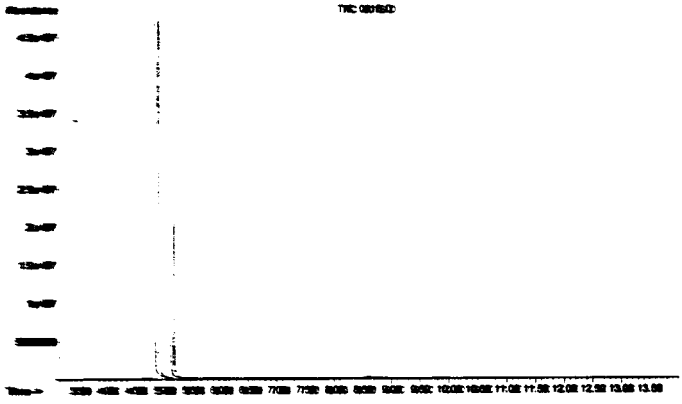

Figure 8. *Gas chromatogram of Reaction 1 at completion.*

In Figure 8, the product is the peak at ~4.8 min in the chromatogram while the excess ethyl 4-bromobutyrate is the peak at about ~5.2 min. Identification of the product was done using the mass spectrum seen in Figure 9. The 280 molecular ion peak that would match the molecular weight of ethyl 1-(4-ethoxy-4-oxobutyl)-2-oxocyclopentanecarboxylate is very small in the spectrum; however, the fragment peaks 242, 224, and 156 were used for identification and are the same as those reported by Nicanon and Kray.[9]

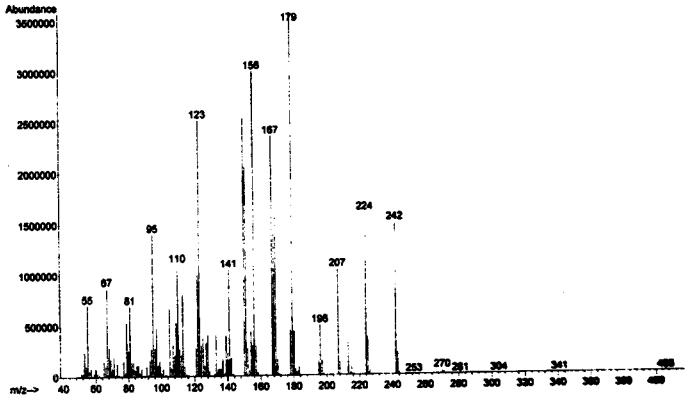

Figure 9. *Mass spectrum of ethyl 1-(4-ethoxy-4-oxobutyl)-2-oxocyclopentanecarboxylate.*

An ^{1}H NMR spectrum of ethyl 1-(4-ethoxy-4-oxobutyl)-2-oxocyclopentanecarboxylate was also obtained, but because of the presence of the ethyl 4-bromobutyrate, the spectrum is difficult to obtain clear data from. The IR spectrum for the product showed a strong peak at 1725 cm^{-1} that confirmed the presence of the carbonyl.

4-(2-Oxocyclopentyl)butanoic Acid: Synthesis and Identification

Reaction 2 involved refluxing the crude 4-(1-ethoxycarbonyl-2-oxoxylopentyl)butanoate from Reaction 1 in aqueous hydrochloric acid to form the 4-(2-oxocyclopentyl)butanoic acid.[9]

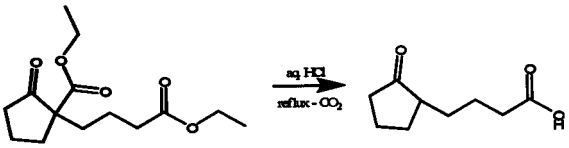

Reaction 2. *Synthesis of 4-(2-oxocyclopentyl)butanoic acid.*

The first mechanistic step of this reaction is the acid hydrolysis of both the ester groups to carboxylic acids. Following this conversion, the carboxylic acid beta to the ketone undergoes decarboxylation resulting in the loss of carbon dioxide and the formation of the desired 4-(2-oxocyclopentyl)butanoic acid.

The setup for this reaction was relatively simply, and like the previous reaction, this reaction can be monitored for completion using GC-MS. In most cases, the gas chromatogram for this reaction was showing one more peak than was expected. This additional peak was the ethyl ester of the desired product. We discovered that this contaminant could be removed by distilling off a portion of the solvent following the reaction. This allowed for the selective conversion of the impurity to the desired product because of the selective removal of ethanol from the reaction mixture.

The chromatogram shown in Figure 10 was taken after distillation and much of the impurity had been removed. The very small peak at ~5.85 min corresponds to the impurity sometimes present. Figure 11 shows the mass spectrum consistent with the formation of 4-(2-oxocyclopentyl)butanoic acid based on the molecular ion peak at 170 and fragments at 152 and 84.

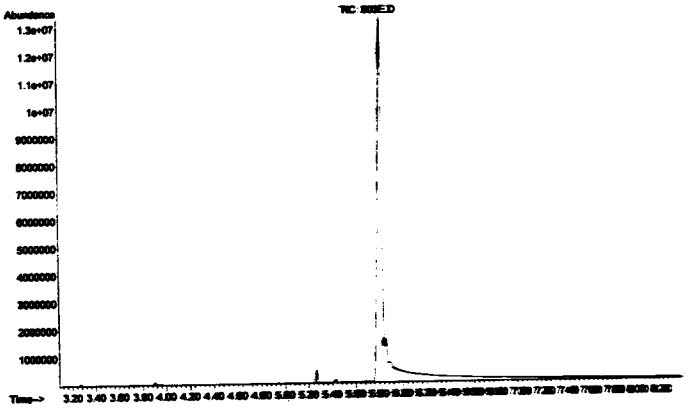

Figure 10. *Gas chromatogram of Reaction 2 at completion.*

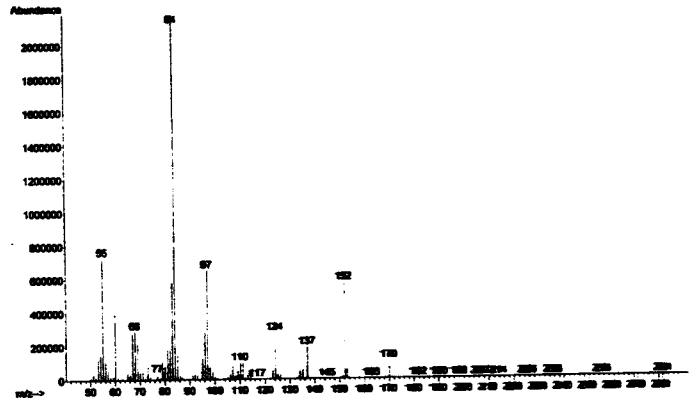

Figure 11. *Mass spectrum of 4-(2-oxocyclopentyl)butanoic acid.*

Spiro[4.4]-nonan-1,6-dione: Synthesis and Identification

The third reaction involved the cyclization of the 4-(2-oxocyclopentyl)butanoic acid to the spiro[4.4]-nonan-1,6-dione in the presence of para-toluenesulfonic acid monohydrate in toluene.[9]

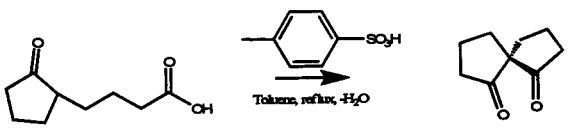

Reaction 3. *Synthesis of spiro[4.4]-nonan-1,6-dione.*

This reaction proceeds through an intremolecular cyclization. Similar to Reaction 1, the mechanism involves reaction α to the ketone. Unlike Reaction 1, the α-carbon react as an enol instead of as an enolate. The enol formation is acid-catalyzed by the para-toluenesulfonic acid. This carbon can attack the carbonyl carbon of the acid (Figure 12). However, it is likely an oxonium ion forms at that carbon through the loss of H_2O prior to the attack.

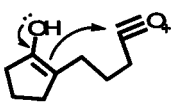

Figure 12. *Attack on carbonyl carbon to form spirodiketone.*

The first step in this synthesis involves dissolving the 4-(2-oxocyclopentyl)butanoic acid in toluene and then using the rotovap to remove some of the solvent. This step was particularly important because traces of ethanol (present from the previous step) will lead to the formation of the ethyl ester of the starting acid. The formation of pure diketone was much easier when this third reaction was done with the purest possible starting material. Reaction 3 could be monitored for completion by either GC-MS or by theoretical loss of water. The latter was done by determining the amount of water that would be lost had all of the starting material reacted and then measuring this

amount using the Dean-stark trap. Following the workup of this reaction, crude brown oil was obtained. To obtain the white solid that the diketone was reported to be, the brown oil was distilled using a short path distillation apparatus.[9] On the twenty gram scale that Reactions 1-3 were done on, a respectable overall yield of 48% was obtained.

As mentioned, GC-MS was used to monitor the completion of the reaction. The spirodiketone came at about ~4.9 min in the chromatogram. When checking the distilled solid, this peak was the only one present. The mass spectrum resulted in a relatively large molecular ion peak at 152 and a fragment peak at 97. Although this GC-MS was used for the initial analysis of the product, ^{1}H NMR was also very useful.

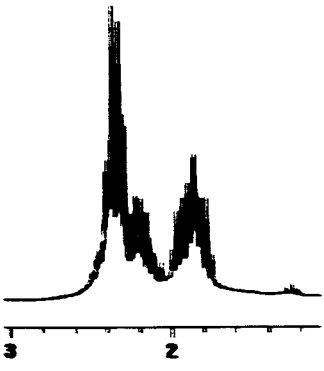

Figure 13. *Upfield region ^{1}H NMR of spiro[4.4]-nonane-1,6-dione.*

The ^{1}H NMR spectrum of the spirodiketone is the first time we got to see the upfield multiplet from the spiro[4.4]nonane group. This distinctive grouping of multiplets seen in Figure 13 is present in all of the ^{1}H NMR spectra of the molecules we synthesized containing the spiro[4.4]nonane group. As expected with the spirodiketone which has no aromatic, amine, or methine hydrogens, there are no peaks further downfield than ~2.5 ppm. This ^{1}H NMR was particularly important because it served as a reference for the ^{1}H NMR spectra taken all of the compounds synthesized after the spirodiketone.

***B*-*n*-butyl oxazaborolidine: Synthesis**

The synthesis of *B*-*n*-butyl oxazaborolidine was carried out as published by Corey *et al.*[10] For this synthesis, we ordered a special Dean-stark trap-like piece of glassware. Because of the small scale of these syntheses, the trap of this piece of glassware was filled with solvent to the bend. This allowed for proper recondensing of the solvent while still allowing for the removal of water. Unlike the published procedure once we isolated the catalyst, we did not prepare solutions of it until it was needed for Reaction 4.

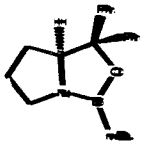

Figure 14. *B-n-butyl oxazaborolidine*

(1*S*,5*R*,6*S*)-Spiro[4.4]-nonan-1,6-diol: Synthesis and Identification

The synthesis of the (1*S*,5*R*,6*S*)-spiro[4.4]-nonan-1,6-diol also referred to as the *trans,trans*-spirodiol was done by using a Corey, Bakshi, and Shibata (CBS) reduction procedure using the *n*-butyl substituted oxazaborlidine catalyst we synthesized.[11]

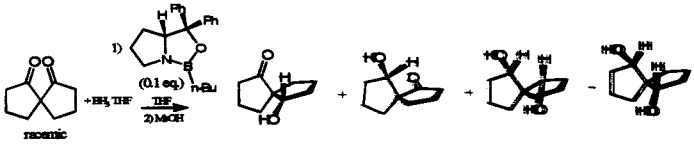

Reaction 4. *Synthesis of (1S,5R,6S)-Spiro[4.4]-nonan-1,6-diol.*

The use of a chiral catalyst in the CBS reduction procedure allowed for the formation of only one stereoisomer from each enantiomer of the spirodiketone. When the racemic chiral spirodiketone is reduced with borane-THF in the presence of the catalyst

the *cis,trans*-spirodiol is the major product; however, when we employed the chiral catalyst, we found the major product to be the desired *trans,trans*-spirodiol. As reported by Lin *et al.*, we sometimes found the monoketone-monodiol product would form in minimal yield, but this side product was easily separated from the *trans,trans*-spirodiol.

We determined that it was important to add the spirodiketone dissolved in THF to the catalyst and borane-THF solution slowly in the synthesis of the spirodiol. When this procedure was done quickly or the reagents added in different orders, there were problems with the reaction. One problem that was sometimes encountered was the incomplete reduction of the spirodiketone. Another problem was that a product was still bound to the *B-n*-butyl group would form. Both of these problems were identified using GC-MS. Also, although it was reported that lowering the temperature significantly decreased the amount of the *cis,trans*-spirodiol formed, we found the difficulty of maintaining the extreme temperatures was not worth the minimal, if even noticeable, decrease in *cis,trans*-spirodiol.

Initial procedures used to isolate the *trans,trans*-spirodiol involved column chromatography. Following the methanol quench, the crude product would be concentrated and using a 9:1 methylene chloride to methanol eluent. The yields obtained for the *trans,trans*-spirodiol using chromatography were discouraging. It is also somewhat difficult to see the *trans,trans*-spirodiol on TLC plates as it chars very slowly. Although, when the *trans,trans*-spirodiol is successfully separated it is quite obvious. The *trans,trans*-spirodiol forms a fluffy white crystalline solid upon removal of solvent, and the *cis,trans*-spirodiol forms a clear oil. If the *trans,trans*-spirodiol is contaminated with any *cis,trans*-spirodiol the white solid that forms is more chalk-like. A ^{1}H NMR of

the pure *trans*,trans-spirodiol can be seen in Figure 15. Another problem that occurred when using this procedure to isolate the spirodiol was that the spirodiol would complex and elute with the catalyst especially when a higher preparation of catalyst were used. Because of low yields and difficulty in purification, we tried alternative methods to get from the spirodiketone to the spirodiamine.

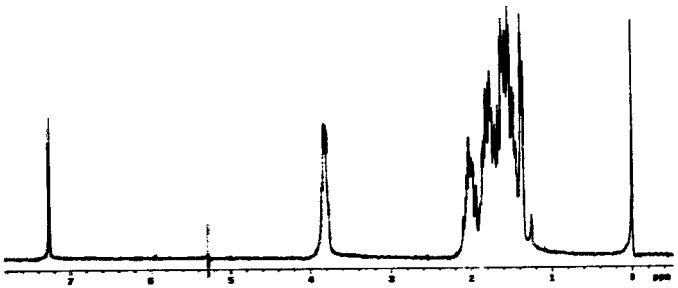

Figure 15. *^{1}H NMR of (1S,5R,6S)-Spiro[4.4]-nonan-1,6-diol.*

A synthetic route was also attempted to convert the ketones to oximes and then to reduce the oximes to amines. The initial studies for this route were done using 4-t-butylcyclohexanone because it was readily available. The conversion of the ketone to the oxime was done by dissolving the methanol and adding hydroxylamine hydrochloride and triethylamine. The reaction was easy and gave great yields.

The first attempt to reduce the oxime was done using nickel boride (Ni_2B). We attempted eight different workups and found no amine product on multiple reaction

attempts. The next reduction attempted was with $LiAlH_4$. The GC-MS of this reaction showed mostly starting material with very little amine formation. A final reduction with $TiCl_4$ and $NaBH_4$ was attempted on the oxime and once again only a very small amount of amine was formed. Although the oxime-route formation initially seemed promising, this route was given up due to the difficulty in reducing the oximes once they were formed. After these attempts, we returned to our initial procedure involving the synthesis of the *trans,trans*-spirodiol.

It was when we returned to the synthesis of the *trans,trans*-spirodiol that we desided to remove the catalyst immediately after the methanol quench. We did this by dissolving the crude product in ethyl acetate and adding 3 M hydrochloric acid that precipitates the hydrochloride salt of the amino alcohol form of the oxazaborolidine catalyst. Following the removal of the catalyst and concentration of the crude product, we dissolved the product in methylene chloride. We knew from previous work with the *trans,trans*-spirodiol that it is relatively insoluble in methylene chloride, and as we suspected the *trans,trans*-spirodiol crystallized out of solution. It should be noted though that recrystallization is sometimes needed to obtain highly pure *trans,trans*-spirodiol.

Figure 16 shows the X-ray crystal structure of the *trans,trans*-spirodiol crystals. The hydrogen bonding between two spirodiol molecules is depicted as a green dotted line in the Figure. The structure along with the distinct

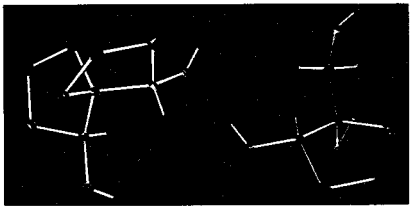

Figure 16. *X-ray crystal structure of (1S,5R,6S)-spiro[4.4]-nonan-1,6-diol.*

[redacted] signal that is shifted downfield around ~3.8 ppm due to the adjacent alcohol group and the typical multiplet grouping upfield in the ^{1}H NMR spectrum (Figure 14) [redacted] that we did in fact isolate the *trans,trans*-spirodiol.

[redacted]-spiro[4.4]-nonane-1,6-dimesylate: Synthesis and Identification

Reaction 5 involves the conversion of the (1*S*,5*R*,6*S*)-spiro[4.4]-nonan-1,6-diol to the (1*S*,5*R*,6*S*)-spiro[4.4]-nonane-1,6-dimesylate with mesyl chloride and TEA in THF.[12]

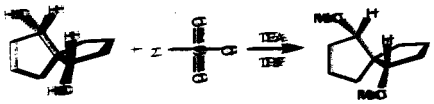

Reaction 5. *Synthesis of (1S,5R,6S)-spiro[4.4]-nonan-1,6-dimesylate.*

This reaction involves the deprotonation of the alcohol groups of the *trans,trans*-spirodiol by triethylamine. This makes the oxygens very nuclephillic, and they displace the chloride group of the mesyl chloride. The mesylate groups are very good leaving groups and important for the azide displacement that follows.

In the synthesis of the spirodimesylate, it is very important to keep the reaction at 0 °C and to add the mesyl chloride *very* slowly. When both the temperature and addition are done correctly, a white solid is obtained following the workup. When these conditions are not maintained, a yellow oil is obtained. In some cases, the yellow oil, which confirmed by TLC, was still pure enough to carry on for the azide displacement reaction, but obtaining a white solid was an excellent sign that pure spirodimesylate was synthesized.

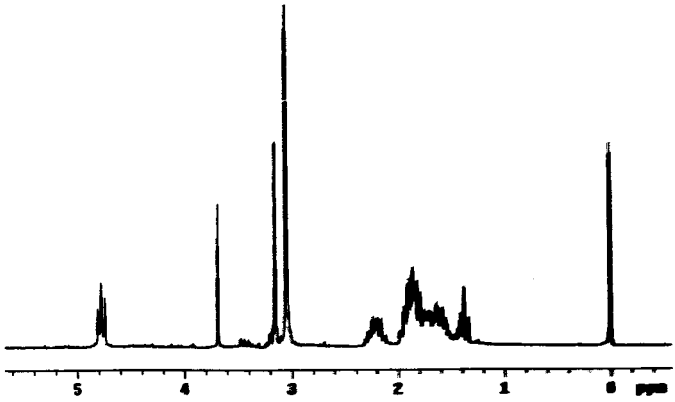

Figure 17. *^{1}H NMR of (1S,5R,6S)-spiro[4.4]-nonan-1,6-dimesylate.*

The spirodimesylate was identified using ^{1}H NMR. There were three distinguishing areas for the spirodimesylate 1) the methine triplet (4.8 ppm), 2) the spiro[4.4]nonane multiplets (3.1 ppm), and 3) the mesylate methyl multiplet (1.7 ppm). The ^{1}H NMR in Figure 17 also shows peaks for the residual mesyl chloride (3.7 ppm) and TEA (2.3 and 1.4 ppm).

(1*R*,5*R*,6*R*)-Spiro[4.4]-nonan-1,6-diazide: Synthesis and Identification

For the sixth step of the synthesis, (1*S*,5*R*,6*S*)-spiro[4.4]-nonan-1,6-dimesylate in DMSO is reacted with sodium azide to yield the products seen in Reaction 6.[12]

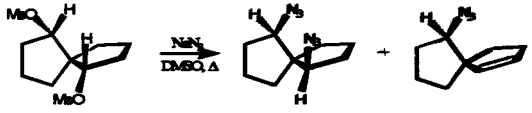

Reaction 6. *Synthesis of (1R,5R,6R)-spiro[4.4]-nonan-1,6-diazide.*

The (1*R*,5*R*,6*R*)-spiro[4.4]-nonan-1,6-diazide product is the result of a double bimolecular nucleophillic substitution (S_N2) reaction. The S_N2 nature of this reaction is responsible for inverting but not interconverting the stereochemistry of the compound. The characteristics of the azide group, small and nuclephillic, and the great mesylate leaving group are necessary to carry out the displacement on the hindered neopentyl-like carbon. The side product monoaizde-monoalkene product forms from a single elimination that is in competition with the substitution.

This reaction was originally carried out in DMF; however, it was determined that the reaction in DMSO went to completion faster and resulted in fewer side products. Unlike many of the previous reactions that were monitored for completion using GC-MS, this reaction is best monitored by either using TLC or running the reaction in d_6-DMSO and checking with ^{1}H NMR. The extraction for this reaction is relatively difficult because of the brown gelatinous substance that hangs at the interface of the organic and aqueous phases. It was determined that this substance did not contain the desired spirodiazide product, but it makes cleanly separating the phases more difficult. It is thought that the spirodiazide is somewhat temperature sensitive, and it is therefore important to use caution when removing the solvent.

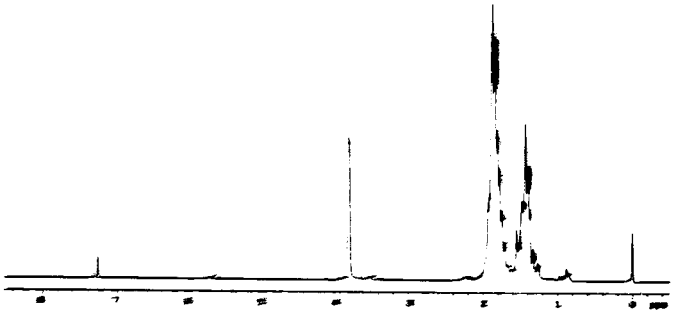

Figure 18. ^1H NMR of (1R,5R,6S)-spiro[4.4]-nonane-1,6-diazide

For the spirodiazide, there were two distinguishing areas of the ^1H NMR (Figure 18). Once again, the typical spiro[4.4]nonane multiplets are seen upfield, and the spirodiazide methine signal came at 3.8 ppm in the ^1H NMR. Determining the purity of the spirodiazide was easily done using ^1H NMR spectroscopy. The monoazide/ monoalkene product had distinct peaks shifted downfield (5.7 and 5.8 ppm) due to hydrogens on the sp^2 carbons of the alkene.

(1R,5R,6S)-Spiro[4.4]nonane-1,6-diamine Synthesis

The formation of the (1R,5R,6S)-spiro[4.4]-nonane-1,6-diamine was done through a standard hydrogenation using a palladium on carbon catalyst and molecular hydrogen as depicted in Reaction 7.[1]

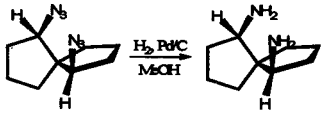

Reaction 7. *Synthesis of (1R,5R,6R)-spiro[4.4]-nonan-1,6-diamine.*

This reaction was done originally only on a very small scale. Yields were relatively low, but no side products have been present, so as expected the scaled up reaction yield improved significantly. Also, the spirodiamine is thought to have a low enough boiling point to cause concern when removing solvent, so because of this, complete solvent removal has not been possible.

SNIP Ligand: Synthesis and Identification

The reaction of the (1*R*,5*R*,6*R*)-spiro[4.4]-nonan-1,6-diamine with 2-hydroxybenzaldehyde results in the standard tetradentate ligand frame as seen in Reaction 8.

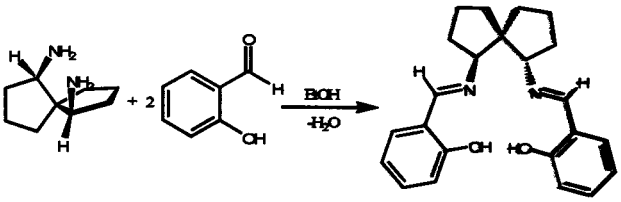

Reaction 8. *Synthesis of SNIP ligand.*

As with the previous synthesis, the yields for this step were lower than expected. This is probably due to the inaccuracies in the number of moles of starting material. The reaction has been carried out twice on small scales and once on a larger scale. In all

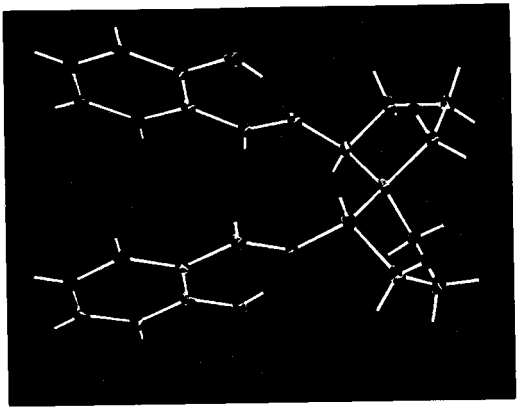

Figure 19. *X-ray crystal structure of SNIP ligand.*

cases, ^1H NMR showed an excess of unreacted 2-hydroxybenzaldhyde suggesting there was less spirodiamine present than measured most likely because of incomplete solvent removal as mentioned previously. This reaction is simple and works well. The product is very symmetric and forms spindly yellow crystals that are easily isolated. These crystals were used to determine the x-ray crystal structure of the SNIP ligand seen in Figure 19.

Future Work

Initial work will include the synthesis of the metal complexes including those of manganese (III), cobalt (II), and chromium (III). Then these complexes will need to be characterized and tested for their reactivity and selectivity in reactions such as chiral epoxidations and selective epoxides ring openings.

In the future, we plan the following alteration to the chiral metal complexes:

a) varying the donor group of the benzaldehyde, starting with phenol and then replacing the hydroxyl with a thiol, a phosphorous, or an amine.

b) Adding bulk to the aromatic rings by adding *t*-butyl groups to the 3- and 5-positions

c) Modifying the spiro backbone of the ligand.

C_2 symmetry is clearly an important part in the catalyst design and will be conserved as we make changes to our complexes. Subsequent systematic changes on the ligand should offer insight into the geometrical requirements at the metal center, which govern specificity. After studying the reactivity of the ligand metal complexes, we hope to identify the contributions of the groups being systematically changed to gain a better understanding of the reactivity and selectivity of chiral C_2 symmetric transition metal complexes as catalysts.

APPENDIX A

Table of Contents

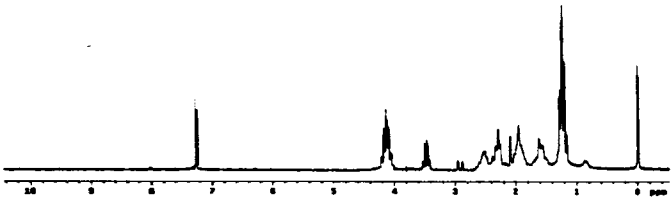

Figure A-1. ^{1}H NMR of Ethyl 1-(4-ethoxy-4-oxobutyl)-2-oxocyclopentanecarboxylate.

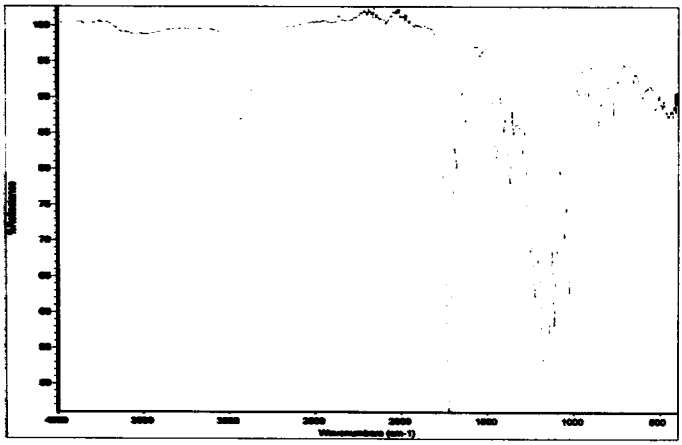

Figure A-2. IR of Ethyl 1-(4-ethoxy-4-oxobutyl)-2-oxocyclopentanecarboxylate.

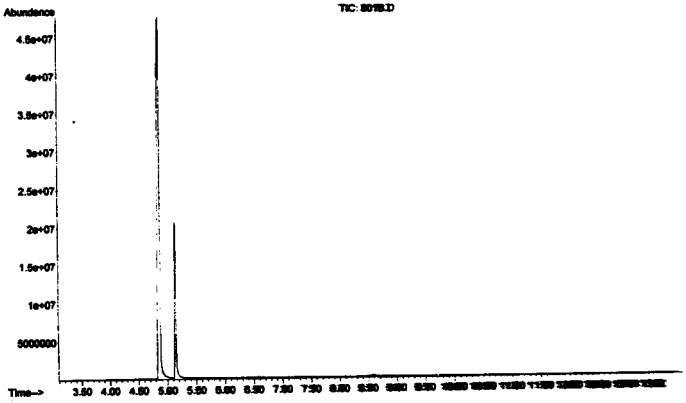

Figure A-3. GC of Ethyl 1-(4-ethoxy-4-oxobutyl)-2-oxocyclopentanecarboxylate

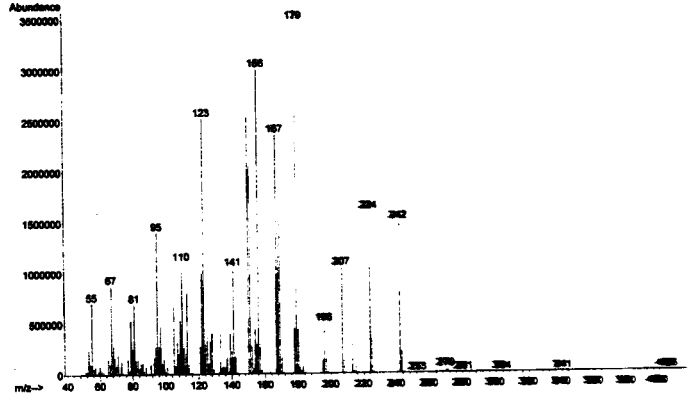

Figure A-4. MS of Ethyl 1-(4-ethoxy-4-oxobutyl)-2-oxocyclopentanecarboxylate

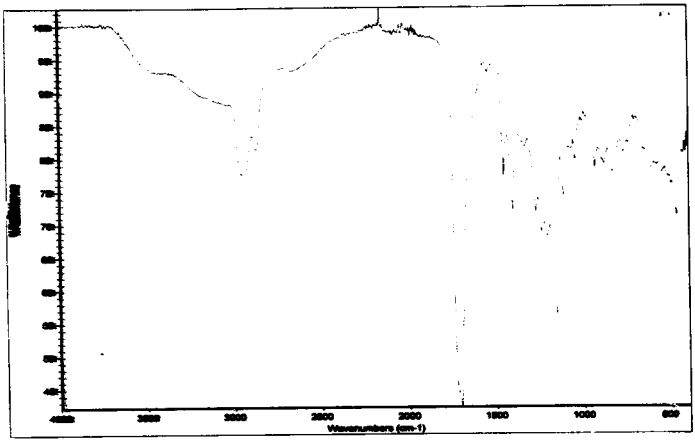

Figure A-5. IR of 4-(2-Oxocyclopentyl)butanoic acid.

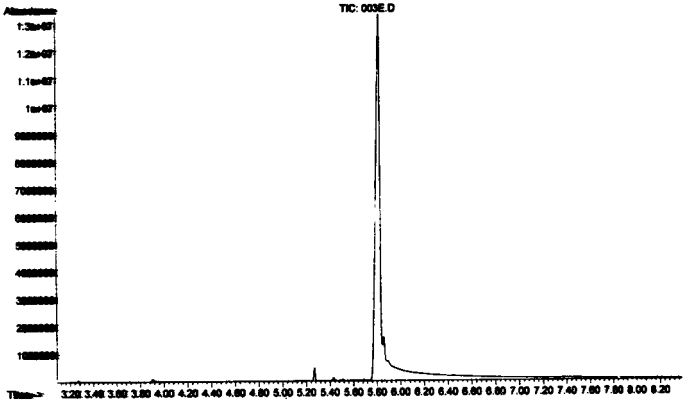

Figure A-6. GC of 4-(2-Oxocyclopentyl)butanoic acid.

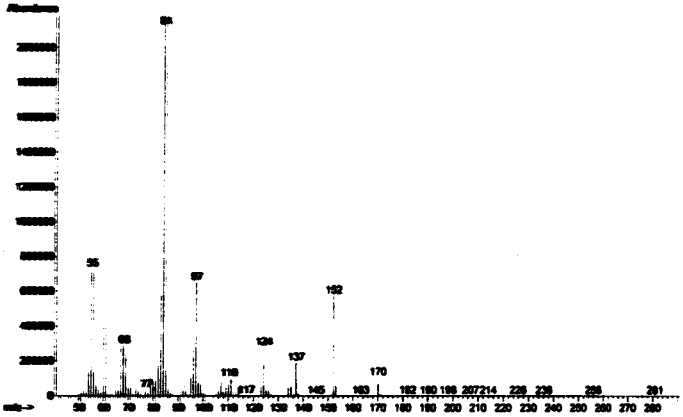

Figure A-7. MS of 4-(2-Oxocyclopentyl)butanoic acid.

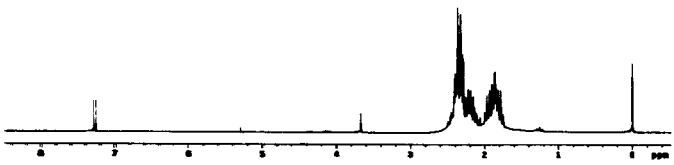

Figure A-8. ^{1}H NMR of Spiro[4.4]-nonan-1,6-dione.

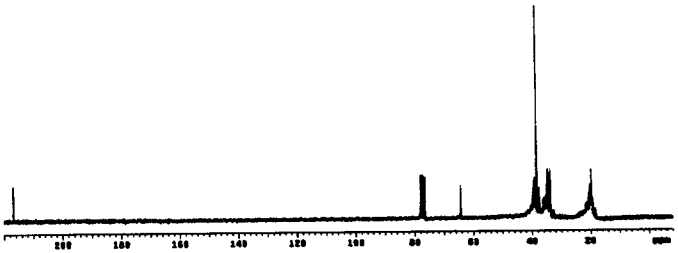

Figure A-9. ^{13}C NMR of Spiro[4.4]-nonan-1,6-dione.

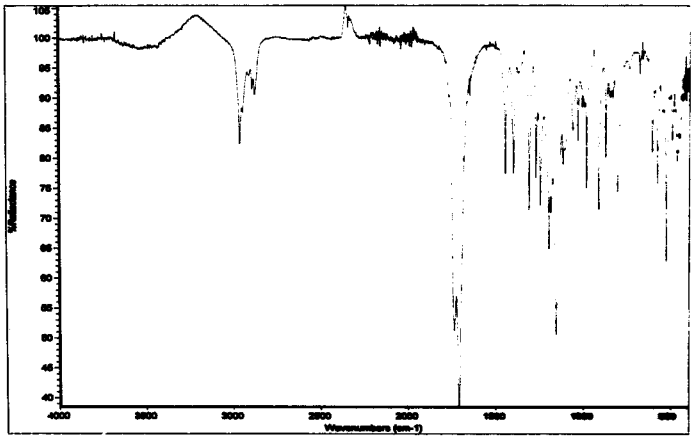

Figure A-10. IR of Spiro[4.4]-nonan-1,6-dione.

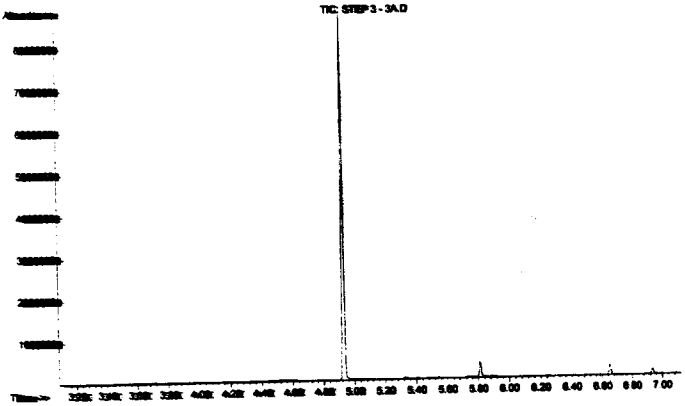

Figure A-101. GC of Spiro[4.4]-nonan-1,6-dione.

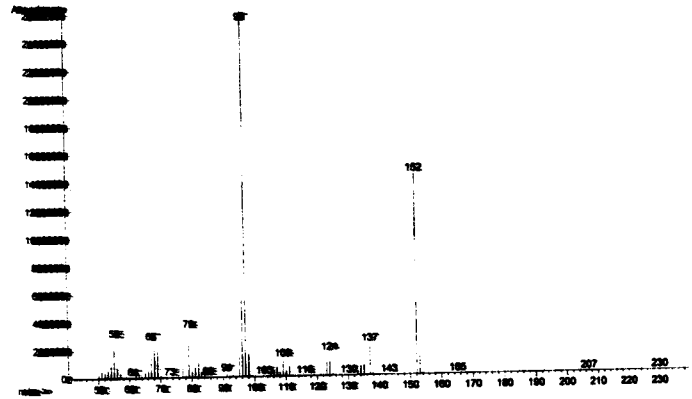

Figure A-102. MS of Spiro[4.4]-nonan-1,6-dione.

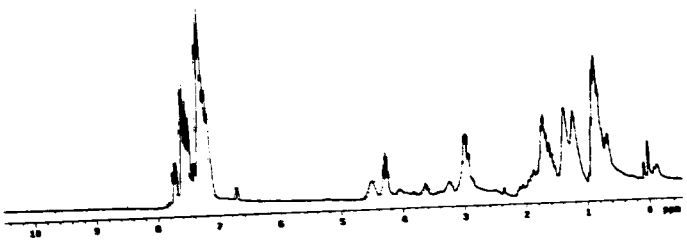

Figure A-13. ^{1}H NMR of *B*-*n*-butyl oxazaborolidine.

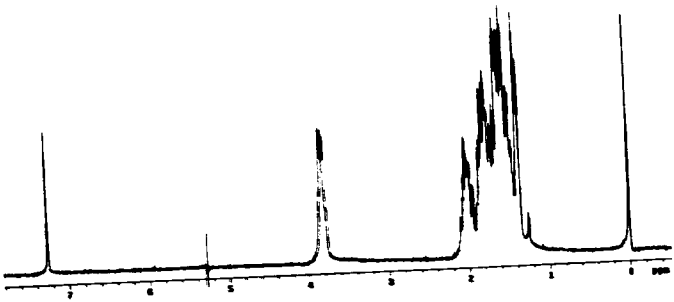

Figure A-14. ^{1}H NMR of (1*S*,5*R*,6*S*)-Spiro[4.4]-nonan-1,6-diol.

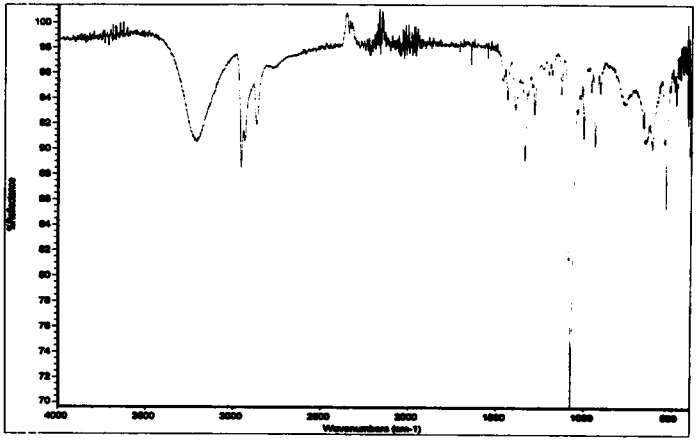

Figure A-15. IR of (1*S*,5*R*,6*S*)-Spiro[4.4]-nonan-1,6-diol.

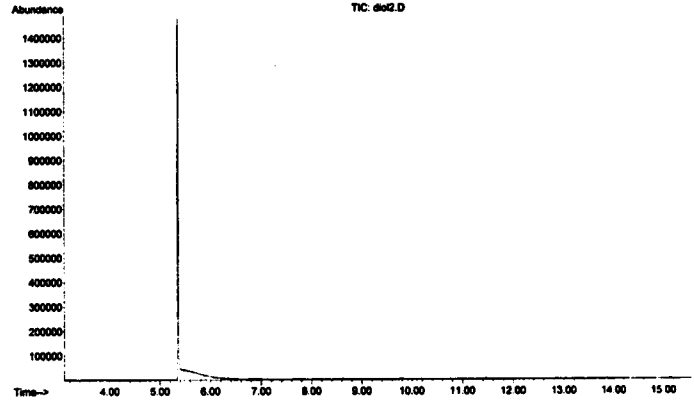

Figure A-16. GC of (1*S*,5*R*,6*S*)-Spiro[4.4]-nonan-1,6-diol.

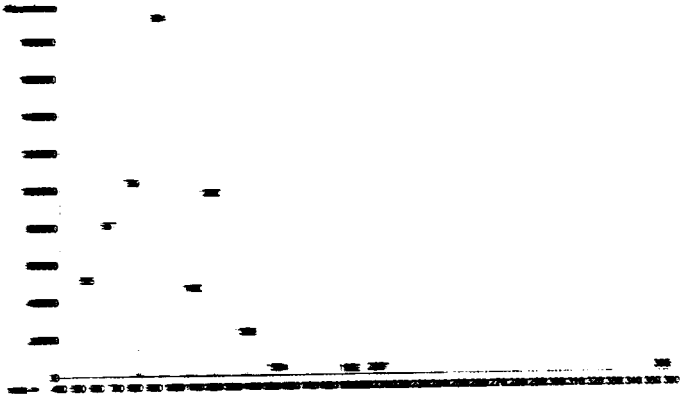

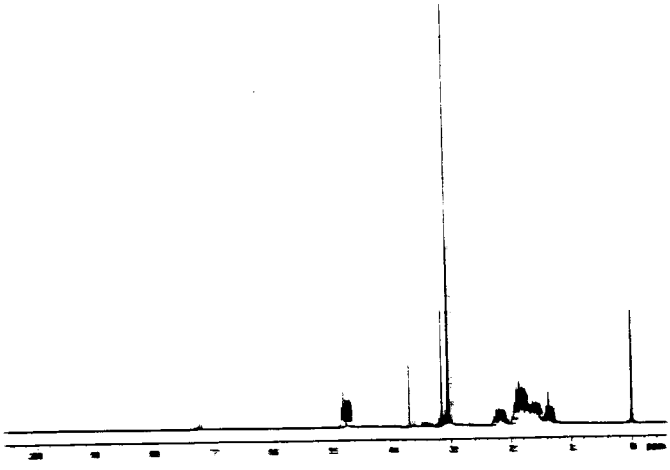

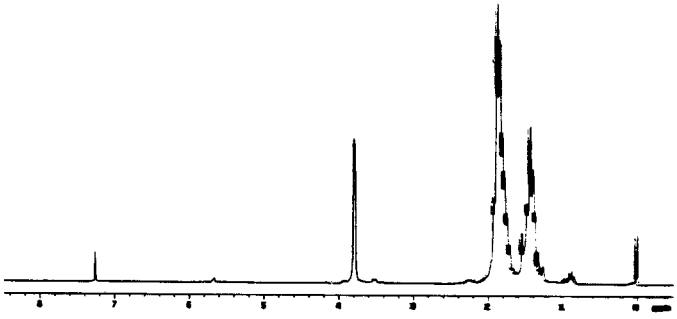

Figure A-19. ^{1}H NMR of (1*R*,5*R*,6*R*)-Spiro[4.4]-nonan-1,6-diazide.

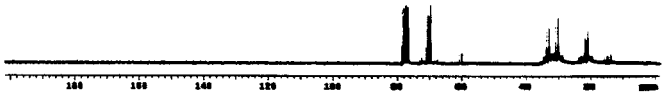

Figure A-20. ^{13}C NMR of (1*R*,5*R*,6*R*)-Spiro[4.4]-nonan-1,6-diazide.

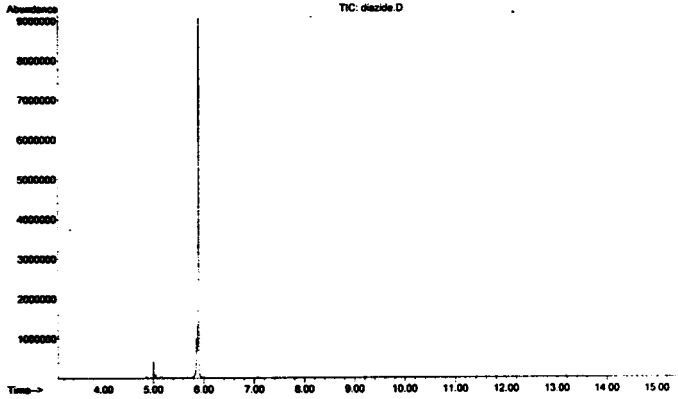

Figure A-21. GC of (1*R*,5*R*,6*R*)-Spiro[4.4]-nonan-1,6-diazide.

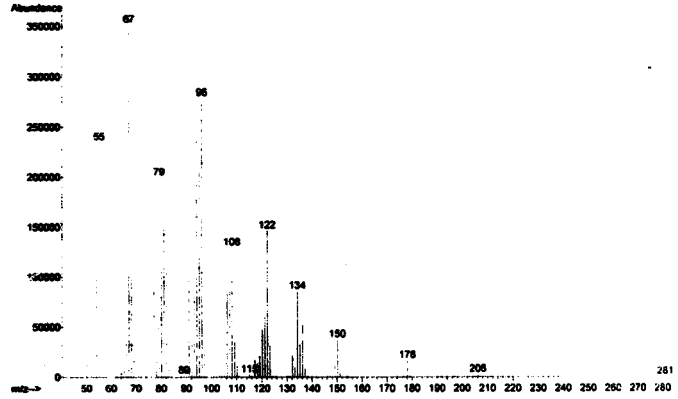

Figure A-22. MS of (1*R*,5*R*,6*R*)-Spiro[4.4]-nonan-1,6-diazide.

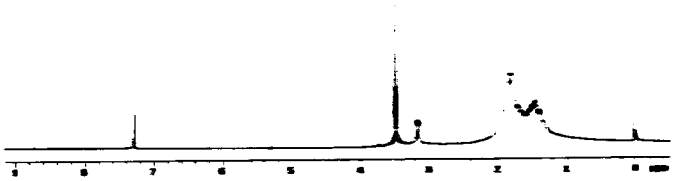

Figure A-23. ^{1}H NMR of (1*R*,5*R*,6*R*)-Spiro[4.4]-nonane-1,6-diamine.

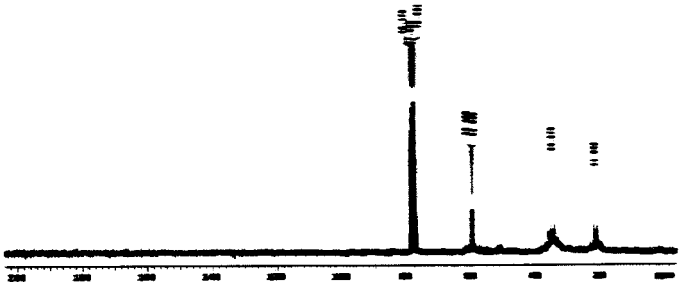

Figure A-24. ^{13}C NMR of (1*R*,5*R*,6*R*)-Spiro[4.4]-nonane-1,6-diamine.

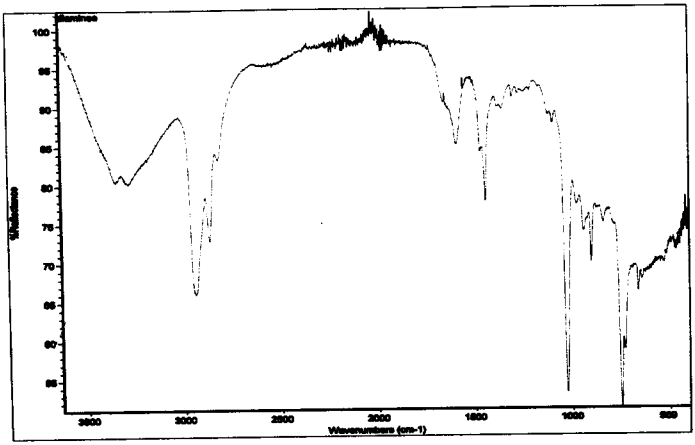

Figure A-25. IR of (1*R*,5*R*,6*R*)-Spiro[4.4]-nonan-1,6-diamine.

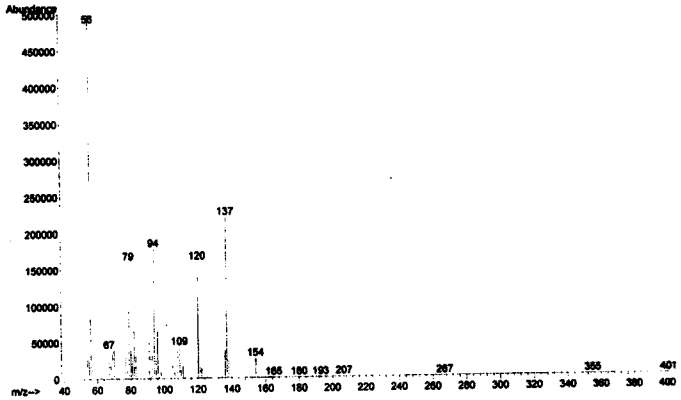

Figure A-26. MS of (1*R*,5*R*,6*R*)-Spiro[4.4]-nonan-1,6-diamine.

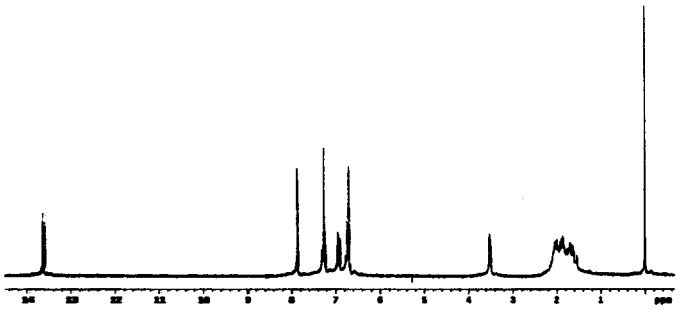

Figure A-27. ^{1}H NMR of SNIP ligand.

REFERENCES

1 Kungl. Vetenskapsakademien, The Royal Swedish Academy of Sciences. Advanced information on the Nobel Prize in Chemistry 2001.

2 Knowles, W. S.; Sabacky, M. J.; Vineyard, B. D.; Weinkauff, D. J. *J. Am. Chem. Soc.* **1975**, 97: 2567-2568.

3 Noyori, R.; Ohta, T.; Takaya, H.; Kitamura, M.; Nagai, K. *J. Org. Chem.* **1987**, 52: 3176-3178.

4 Sharpless, K. B.; Rossiter, B. E.; Katsuki, T. *J. Am. Chem. Soc.* **1981**, 103: 464-465.

5 Zhang, W.; Loebach, J. L.; Wilson, S. R.; Jacobsen, E. N. *J. Am. Chem. Soc.* **1990**, 112: 2801-2803.

6 Jacobsen, E. N.; Zhang, W.; Muci, A. R.; Ecker, J. R.; Deng, L. *J. Am. Chem. Soc.* **1991**, 113: 7063-7064.

7 Fristrup, P.; Dideriksen, B. B.; Tanner, D.; Norrby, P.-O. *J. Am. Chem. Soc.* **2005**, 127: 13672-13679.

8 Houk, K. N. *et al*, http://www.ch.ic.ac.uk/ectoc/echet96/papers/198/index.htm

9 Nieman, J. A.; Keay, B. A. *Synthetic Communications*. **1999**, 29: 3829-3840.

10 Corey, E. J., Bakshi, R. K., Shibata, S. *J. Am. Chem. Soc.* **1987**, 109: 5551-5553.

11 Lin, C.-W.; Lin, C.-C.; Li, Y.-M.; Chan, A. S. C. *Tetrahedron Letters*. **2000**, 41: 4425-4429.

12 Lin, C.-W.; Lin, C.-C.; Lam, L. F.-L. ; Au-Yeung, T. T.-L.; Chan, A. S. C. *Tetrahedron Letters*. **2004**, 45: 7379-7381.